# Friction and Abrasion Resistance of Cast Aluminum Alloy–Fly Ash Composites

P.K. ROHATGI, R.Q. GUO, P. HUANG and S. RAY

The abrasive wear properties of stir-cast A356 aluminum alloy-5 vol pct fly ash composite were tested against hard $SiC_p$ abrasive paper and compared to those of the A356 base alloy. The results indicate that the abrasive wear resistance of aluminum–fly ash composite is similar to that of aluminum-alumina fiber composite and is superior to that of the matrix alloy for low loads up to 8 N (transition load) on a pin. At loads greater than 8 N, the wear resistance of aluminum–fly ash composite is reduced by debonding and fracture of fly ash particles. Microscopic examination of the worn surfaces, wear debris, and subsurface shows that the base alloy wears primarily by microcutting, but the composite wears by microcutting and delamination caused by crack propagation below the rubbing surface through interfaces between fly ash and silicon particles and the matrix. The decreasing specific wear rates and friction during abrasion wear with increasing load have been attributed to the accumulation of wear debris in the spaces between the abrading particles, resulting in reduced effective depth of penetration and eventually changing the mechanism from two-body to three-body wear, which is further indicated by the magnitude of wear coefficient.

## I. INTRODUCTION

METAL matrix composites (MMCs) have attracted considerable attention because of our ability to tailor their physical, mechanical, and tribological properties[1–8] for a given application. The composites containing particles have isotropic properties which are attractive to design engineers because of their easy adaptability to current design practice. The possibility of near-net-shape manufacturing using conventional methods makes MMCs more attractive, even from the point of view of manufacturing components. However, the high cost of the presently available MMCs remains a major barrier in their widespread use.

Recently, a new particulate composite containing fly ash, a waste by-product from power plants, has been developed by incorporating these hard particles in molten aluminum alloys. Since fly ash represents an inexpensive resource material, this new composite is likely to overcome the cost barrier for widespread applications in automotive and small engine applications.[9,10,11] Thus, the incorporation of waste fly ash particles in aluminum will promote yet another use of this low-cost waste by-product and, at the same time, has the potential of displacing the energy-intensive aluminum and, thereby, reducing the cost of aluminum products.

Fly ash is a coal combustion by-product consisting primarily of aluminosilicates. Table I shows the typical chemical composition range of fly ash. A comparison of properties of fly ash with other ceramic dispersoids commonly used in MMCs, such as SiC and $Al_2O_3$, demonstrates that many of the constituents of fly ash are much lighter than aluminum and closer to ceramic dispersoids, as shown in Table II.[12] Fly ash particles generally contain either solid spheres called precipitator fly ash or hollow spheres termed cenosphere fly ash. Precipitator fly ash often has pores and its density ranges from 2.1 to 2.6 g/cm$^3$. The particle size of the fly ash as received from the power plants generally lies in the range from 1 to 150 $\mu$m, while cenosphere fly ash particles have sizes ranging from 10 to 250 $\mu$m, with density in the range of 0.4 to 0.6 g/cm$^3$. The wall thickness of a hollow cenosphere is about 10 pct of its diameter. Technology is now available to separate cenospheres from solid spheres and to obtain particles of close chemistry and size from collected fly ash. It is therefore possible to select a suitable fraction of fly ash for incorporation into a metal matrix in order to impart lower density, lower thermal conductivity, higher electrical resistance, or higher damping capacity to the resulting composites to meet specific requirements.[12]

Abrasive wear is a type of wear which leads to a much faster loss of material and dimension, because its wear coefficient is at least one or two orders of magnitude higher than those observed in other modes of wear. In monolithic alloys, it has been observed that wear volume increases rapidly with grit size of abrading particles up to a critical diameter; beyond this size, the wear increases at a slower rate. When the size of the abrading particle is below 1 $\mu$m, the wear is no longer by abrasion.[13] In MMCs, as in monolithic alloys, abrasive wear involves gouging, grooving, and plastic deformation caused by penetration of hard abrading particles.[14] The interaction of abrading particles with the dispersed hard particles, such as fly ash in the composite during abrasion wear, is a feature which is not present during the abrasion of monolithic metals or alloys. The present study involves determination of the abrasive wear in the aluminum casting alloy A356 base composite containing fly ash particles tested against hard SiC abrasive paper and its comparison to that observed in the base alloy. The abrasive wear behavior of the composites has been investigated primarily to understand the nature of interaction between the dispersed fly ash and the abrading particles at high stress at the regions of contact, keeping in mind the

P.K. ROHATGI, Professor, R.Q. GUO, Postdoctoral Fellow, and P. HUANG, Doctoral Student, are with the Department of Materials, University of Wisconsin-Milwaukee, Milwaukee, WI 53201. S. RAY, Professor, is with the Department of Metallurgical Engineering, University of Roorkee, Roorkee, 247 667, India.

Manuscript submitted August 1, 1996.

**Table I. Typical Chemical Composition of Fly Ash, in Weight Percent**

| $Al_2O_3$ | $SiO_2$ | CaO | $Fe_2O_3$ | MgO | $K_2O$ | $Na_2O$ | $TiO_2$ | $SO_3$ | LOI* |
|---|---|---|---|---|---|---|---|---|---|
| 15 to 30 | 30 to 70 | 1 to 5 | 10 to 20 | 0 to 2 | 1 to 5 | 0 to 2 | 0 to 2 | 0 to 2 | 0 to 10 |

*LOI = loss of ignition

**Table II. Physical and Mechanical Properties of Fly Ash Compared to SiC, $Al_2O_3$, and Al**

| Material | True Density ($g/cm^3$) | Melting Point (°C) | Modulus (GPa) | Thermal Conductivity* (W/m·K) | Electrical Resistance (Ohm cm) |
|---|---|---|---|---|---|
| Precipitator fly ash | 2.1 to 2.6 | >1200 | 143 to 310 | 0.06 to 0.16 | $10^9$ to $10^{12}$ |
| Cenosphere fly ash | 0.4 to 0.6 | | | | |
| SiC | 3.2 | — | 420 | 100** 4 to 20† | 1000 |
| $Al_2O_3$ | 3.9 | 2250 | 380 | 100** 5 to 30† | — |
| Al | 2.7 | 660 | 67 to 79 | 237 | $3.15 \times 10^{-6}$ |

*At room temperature
**Single crystal
†Polycrystal

specific characteristics of fly ash particles as presented previously and the major constituent of glassy phase complex compounds.

## II. EXPERIMENTAL PROCEDURE

### A. *Synthesis of Composites and Preparation of Specimen for Wear Test*

The matrix material used for the preparation of the composite for this investigation was the standard A356 casting alloy, and its chemical composition is shown in Table III. A typical micrograph of precipitator fly ash from Wisconsin Electric used in this study is shown in Figure 1.

The composites with 5 vol pct fly ash were synthesized by stir casting into a mold of 50-mm diameter. Pin samples of diameter 6 mm and length 15 mm, machined from the middle of the composite ingots, have been used for the wear tests. Pins of the similarly cast base alloy without any fly ash particle were fabricated for wear tests.

### B. *Abrasion Wear Test*

Abrasion wear tests were carried out on a pin-on-disk type FALEX machine. Pin specimens were rubbed on bonded SiC abrasive papers of different grit sizes. Three pins were mounted, 120 deg apart, on a circle in a holder. The pins were loaded in contact with the abrasive paper fixed on a stationary disc. The applied loads on the samples were 8.9, 17.8, 28.7, and 35.6 N. The rotational speeds of the pins used in the tests reported were 1 and 2 m/s. The SiC grit sizes used were in the range from 240 to 600, corresponding to average particle sizes between 58 and 15 $\mu$m, respectively. The mean track radius of pin samples was observed to be 17 mm. Pin weights were measured before and after each test segment of 5 minutes to determine the abrasive wear loss of each pin. Temperature near the abrasive surface was measured using a thermocouple placed very close (about 2 mm) to the rubbing surface below the abrasive paper.

The specific wear rate (SWR) was calculated by dividing the average pin weight loss, $M$, by the total rubbing distance, $S$, and the load, $L$, on each pin (*e.g.*, one-third of total applied load) as follows:

$$\text{SWR} = M/(S \times L) \quad [1]$$

When $M$ is measured in milligrams, $S$ is determined in meters, and $L$ is given in Newtons, the SWR may be expressed in units of mg/m · N. If one uses volume loss in place of weight loss, SWR may be expressed in units of $cm^3$/m · N. Specific wear resistance is the reciprocal of specific wear rate, and the lower the SWR, the higher the specific wear resistance of the material.

The coefficient of friction was estimated by measuring the torque on the pins, $T$, and the radius of the wear track, $R$, using the following equation:

$$\text{coefficient of friction, } \mu = T/(L \times R) \quad [2]$$

where $L$ is the applied load.

### C. *Accuracy of the Test*

In the abrasive wear tests described, the controlled variables ($X_i$) and the observations ($Y_i$) are as follows. The accuracy of measurement of variables and observations is given subsequently.

1. $X_i$: controlled variables
   - $X_1$—velocity: two levels of 1 and 2 m/s, with accuracy 0.1 pct.
   - $X_2$—load: four levels of 8.9, 17.8, 26.7, and 35.6 N, with accuracy 5 pct.
   - $X_3$—SiC size: four levels of 15, 22, 31, and 58 $\mu$m mean size (*i.e.*, grit nos. 240, 320, 400, and 600), with accuracy 5 pct.
   - $X_4$—time, one level, 5 minutes, with accuracy 0.5 pct.
2. $Y_i$: observations
   - $Y_1$—weight loss; milligram, with accuracy 0.1 mg.
   - $Y_2$—temperature rise; °C, with accuracy 1 °C.
   - $Y_3$—specific wear rate; mg/m · N, with accuracy 5 pct.
   - $Y_4$—torque; N · m, with accuracy 0.01 N · m.

### D. *Examination of Worn Surfaces, Subsurfaces, and Wear Debris*

The worn surfaces of pins and SiC abrasive paper and wear debris were examined using a scanning electron mi-

**Table III. Chemical Composition of A356 Al-Si-Mg Alloy, in Weight Percent**

| Si | Mg | Cu | Fe | Ti | Mn | Zn | Al |
|---|---|---|---|---|---|---|---|
| 6.50 to 7.50 | 0.25 to 0.45 | 0.10 | 0.20 | 0.20 | 0.20 | 0.10 | balance |

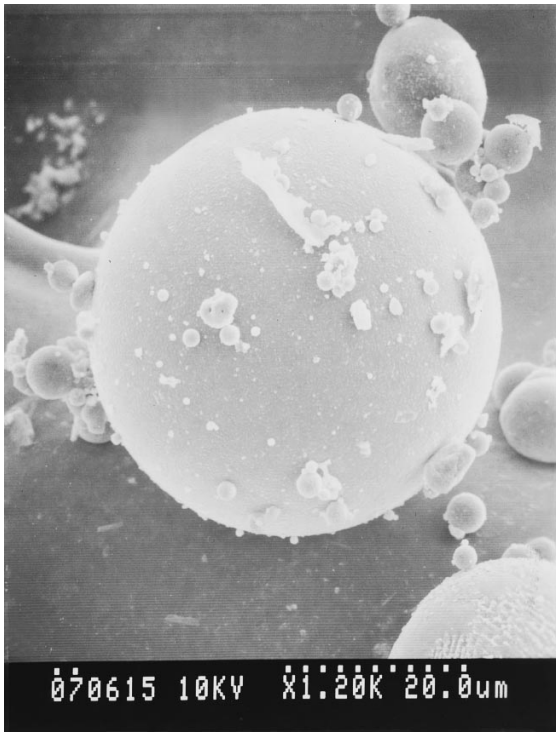


Fig. 1—SEM micrograph showing the spherical shape of fly ash particles.

croscope (SEM). The surface of the test samples was cleaned ultrasonically in a medium of acetone and coated with a thin film of gold before examination under the SEM. For subsurface examination under an optical microscope, the test pins were mounted in polymers after the wear test and the transverse section was prepared by grinding and polishing.

## III. RESULTS AND DISCUSSIONS

### *Characterization of Composite*

The microstructure of Al alloy–fly ash composite is shown in Figure 2. The fly ash particles are generally present near the last to freeze interdendritic regions of the solidification microstructures of the matrix alloy. This segregation of fly ash in the interdendritic regions is presumably due to lack of nucleation of $\alpha$-aluminum dendrites on the surface of fly ash and the pushing of fly ash particles by the growing $\alpha$-aluminum dendrites during solidification. Similar pushing of reinforcement particles is observed during solidification of Al-SiC and Al-$Al_2O_3$ composites.[15] Table IV shows the average density and the average hardness of the composite and those of the matrix alloy. With 5 vol pct of fly ash, the density of composite decreases to 2.58 g/cm$^3$ compared to the density of aluminum alloy 2.68 g/cm$^3$. A comparison of the measured density with the one calculated on the basis of density of constituents reveals the

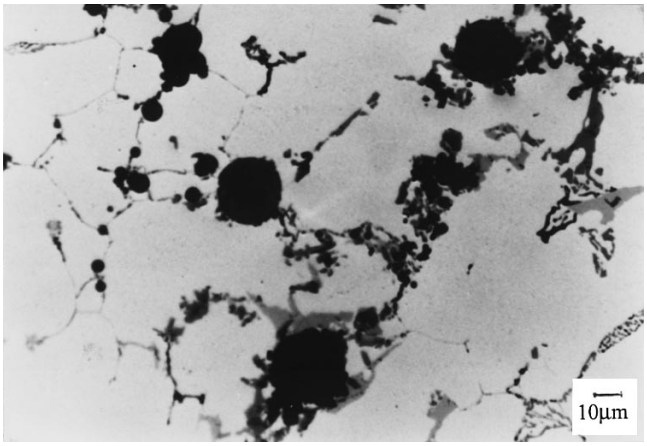


Fig. 2—Optical micrograph showing the distribution of fly ash in the A356 matrix alloy.

**Table IV. Average Density and Average Hardness of the Matrix Alloy and the Composite**

| Material | Volume Percentage of Fly Ash, Pct | Density (g/cm$^3$) | Hardness, HRF (kg/mm$^2$) |
|---|---|---|---|
| A356 alloy | 0 | 2.68 | 79 |
| A356-5 vol pct fly ash | 5 | 2.58 | 82 |

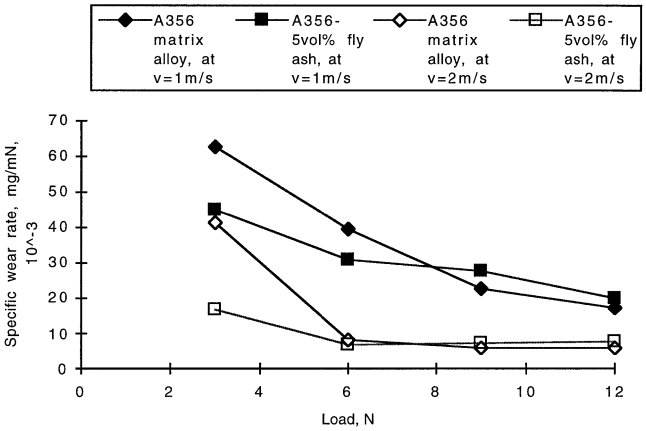


Fig. 3—Specific wear rate *vs* load at $v$ = 1 and 2 m/s; SiC paper = 320 grit (31 $\mu$m); time = 5 min.

presence of about 3 vol pct of porosity. The hardness of the matrix alloy is 79 kg/mm$^2$.

The variation of SWR of the matrix alloy and the Al alloy–fly ash composite with load is shown in Figure 3. It is observed that for both the matrix alloy and the composite, the SWR decreases as the load increases. At a sliding velocity of 1 m/s, the SWR of the composite is lower at loads lower than 8 N (transition load), as compared to the SWR of the matrix alloy. At higher loads greater than 8 N, the SWR of the Al alloy–fly ash composite is slightly higher than that of the Al alloy. The similar results obtained at higher sliding velocities of 2 m/s under the same experimental conditions are also indicated in Figure 3. The transition load at which the wear resistance of the aluminum alloy–fly ash composite becomes lower than the matrix seems to be independent of the sliding velocity. A com-

**Table V. A Comparison of Abrasion Wear Rate in Composite Materials**

| Investigators | Test Configuration | Test Condition | Abrading Particles | Material | Wear Rate ($mm^3/m$) |
|---|---|---|---|---|---|
| Wang and Hutchings[16] | 5-mm diameter pin on rotating disc | $v = 0.63$ ms$^{-1}$<br>$L = 1.9$ N<br>$t = 60$ s | SiC—25 $\mu$m | 6061 Al-10 pct $Al_2O_{3f}$<br>6061 Al | $29.4 \times 10^{-3}$<br>$86.3 \times 10^{-3}$ |
| Alahelisten et al.[17] | block on rotating disc | $P = 0.35$ MPa<br>$v = 1.0$ ms$^{-1}$<br>$t = 20$ s | SiC—15 $\mu$m | Al<br>Al-10 pct $Al_2O_3$<br>Mg<br>Mg-10 $Al_2O_3$ | 20.7<br>0.8<br>2.0<br>1.1 |
| Present authors | pin on disc | $v = 1.0$ ms$^{-1}$<br>$L = 2.97$ N<br>t = 300 s | SiC—31 $\mu$m<br>SiC—31 $\mu$m | A356 alloy<br>A356-5 vol pct fly ash | $70 \times 10^{-3}$<br>$51.3 \times 10^{-3}$ |

parison of abrasion wear of aluminum alloy–fly ash composite with composites containing alumina fibers is shown in Table V.

Examination of the worn surfaces of aluminum–fly ash composites under the SEM after wear test shows that under the load of 2.97 N, the worn surface has relatively less ploughing and cutting, as shown in Figure 4(a). However, at the load of 11.9 N, fractured fly ash particles are frequently present on the worn surface, as shown in Figure 4(b).

Experimental results indicate that the aluminum alloy–fly ash composite shows a lower SWR (higher wear resistance) than matrix alloy at all abrasive particle sizes tested (15 to 58 $\mu$m) at a load of 2.97 N. In A356-5 vol pct fly ash composite, the SWR increases as the abrasive particle size increases, with an abrupt and sharp rise occurring between 22 and 31 $\mu$m (400 and 320 mesh, respectively). There is a slight decrease between 31 and 58 $\mu$m, and this is within the allowable limit of experimental error. At SiC particle sizes between 15 and 22 $\mu$m, the SWR is much smaller than the SWR at 31 and 58 $\mu$m. A large increase (90 pct) in SWR was observed between 22 and 31 $\mu$m. This is very similar to that observed in monolithic materials by Sin *et al.*[18] The wear rate increases rapidly until a critical grit size is reached. Beyond this critical size, the wear rate becomes independent of grit size or increases only slowly. For widely divergent types of materials of polymethyl methacrylate, nickel, and AISI 1095 steel, the maximum change in wear rate has been observed to lie in the range between 20 and 30 $\mu$m of abrading SiC particles, as it has been observed in the present investigation. Wang *et al.*[16] have measured the abrasion wear of 6061 aluminum alloy base MMC reinforced with alumina fibers using the pin-on-disc method by running the specimen on a single track with various grit sizes of abrasive paper. It was found that the wear resistance in this alumina fiber-reinforced composite decreases with increasing size of the abrading particles, as has been observed here in aluminum–fly ash composites.

Figure 5 shows that the aluminum alloy–fly ash composite has a lower coefficient of friction (0.50 to 0.57) than that of the matrix alloy (0.50 to 0.72) under different loads. As the load increases, the coefficient of friction decreases for both the composite and the matrix alloy. The change in friction coefficient with load is a little more than that observed by Sin *et al.*[18] in monolithic materials, such as AISI 1095 steel and nickel. The decrease of the coefficient of friction with the increase of the load may be attributed to increasing amounts of wear debris particles coming out from the wear surface and filling in the empty spaces between SiC particles, thereby decreasing the effective depth of penetration. Since the wear debris particles are loose, they can also start sliding at the interface between the pin material and the abrasive, causing reduced grooving of the

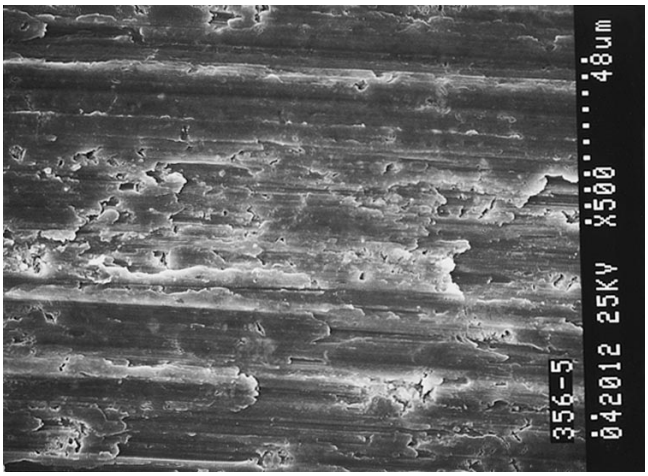


(*a*)

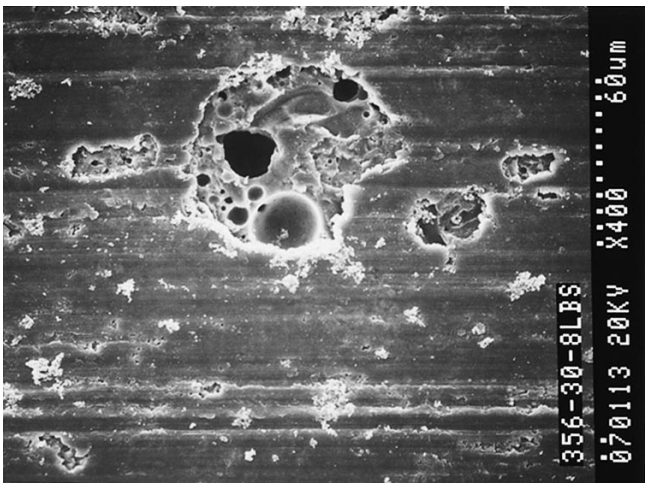


(*b*)

Fig. 4—SEM micrographs of the worn surfaces after the wear test under velocity = 1 m/s; time = 5 min; SiC paper = 320 grit (31 $\mu$m): (*a*) load = 2.97 N and (*b*) 11.9 N.

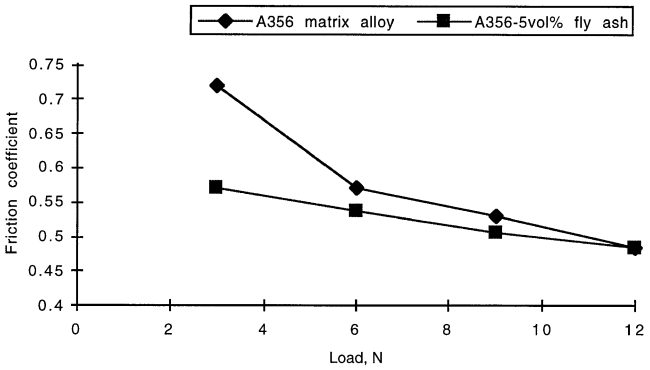


Fig. 5—Coefficient of friction *vs* load at $v = 1$ m/s; SiC paper = 320 grit (31 $\mu$m).

matrix and also decreasing the effectiveness of the cutting force of SiC. The loose debris can get in-between the rubbing surfaces causing the wear mechanism to change from two-body to three-body abrasion. This effect may be more dominant, and so it has been able to obliterate the general trend of an increase in coefficient of friction with load. An indication of the importance of this effect in the abrasion wear rate is evident in Figure 3 from a comparison of SWR data for velocities of 1 and 2 m/s. In the former case of 1 m/s, the SWR is averaged over a shorter sliding distance than that for the latter case. The accumulation of wear debris between the abrading particles has reduced the wear rate more because of larger sliding distance in the case of the sliding velocity of 2 m/s.

The aluminum alloy–fly ash composite also exhibits lower coefficients of friction (0.47 to 0.72) than that of the matrix alloy (0.67 to 0.78) under different particles sizes. As the abrasive particle size increases, the coefficient of friction decreases. However, the coefficient of friction should increase with increasing size of the abrading particles, because the included angle of abrasion increases with increasing grit size,[13] a trend contrary to the present results. This also is attributed to the reduced effective depth of penetration due to accumulation of wear debris. A lower coefficient of friction in the composite as compared to that in the base alloy may be the result of the cracking and delamination of the composite, which were absent in the base alloy.

Microscopic examination of the subsurfaces below the rubbing surfaces of the composite and the base alloy was conducted on transverse sections of the pins after the wear test. It has been observed that the wear in the composite is sometimes accompanied by delamination of the alloy adjacent to the particle. It was observed that the subsurface cracks propagate from the rubbing surface along the interface of silicon particles with the matrix in the composite. However, such cracking along the interface of silicon particles was generally not observed in the base alloy. In this context, it may be important to note that the composite appears to have more silicon in the matrix, sometimes present as large polyhedral silicon, which may be due to chemical reaction of the ash particles with molten aluminum alloy during processing.

The temperature rise at the rubbing interface is a function of the coefficient of friction, distance, velocity, load, and material. Under the test conditions used in this study, the temperature rise at the pin surfaces of the composite and the matrix alloy increases with increasing load and velocity. Compared to the matrix alloy, the composite pins indicate marginally higher rise in temperature (less than 2 °C) under the experimental conditions. Since the coefficient of friction of composites is lower than that observed in the base alloy, total heat generated during the test is expected to be lower for the Al alloy–fly ash composite as compared to that for the base alloy. Therefore, a higher temperature rise could probably be due to the lower thermal conductivity of the composite (as shown in Table II) driving the heat flux toward the disc.

Many previous investigations have been done on two-body abrasive wear in order to develop a fundamental understanding of wear mechanism. A classical model has been expressed by Rabinowicz:[19]

$$dV/dl = kP/H \qquad [3]$$

where

$dV/dl$ = volume loss per unit sliding distance,
$P$ = load applied,
$H$ = hardness, and
$k$ = wear coefficient.

Equation [3] does reveal basic observation in two-body abrasion. Generally, the volume loss of material is proportional to the load and sliding distance and is inversely proportional to the hardness of the surface. The value $k$ can be calculated from Eq. [3], and the calculated $k$ values for both the matrix alloy and the aluminum alloy–fly ash composite under the present experimental conditions are in the range of 1 to 18 $\times$ $10^{-3}$. The typical $k$ values for two-body abrasive wear are in the range 16 to 180 $\times$ $10^{-3}$, and the typical $k$ values for three-body abrasive wear are in the range 2 to 6 $\times$ $10^{-3}$.[19] The $k$ values under the test conditions are very close to the $k$ values of the three-body situation. It is indicated that there is a transition from two-body abrasive wear to three-body abrasive wear due to accumulation of wear debris, because the tests are conducted by sliding again and again on a single wear track.

## IV. CONCLUSIONS

Fly ash, an inexpensive resource material, may be introduced into the A356 aluminum alloy to make a cost competitive composite with a slightly decreased density and a marginally increased hardness. The abrasion wear behavior of the A356 aluminum alloy containing 5 vol pct fly ash sliding on a single track again, and again on SiC abrading particles, is summarized subsequently.

1. The abrasion wear resistance of the alloy containing 5 vol pct fly ash is similar to aluminum alloys containing alumina fibers and is superior to that of the base A356 alloy below a load of 8 N at sliding velocities of 1 and 2 m/s. Above this load, debonding and fracture of fly ash particles may be responsible for increasing the SWR of the composite to a level higher than that of the base alloy.
2. The observed decrease of SWR with an increase in load has been attributed to an accumulation of wear debris in the spaces between the abrading particles, leading to a reduced depth of penetration and an eventual transition

from two-body to three-body wear. This effect is also reflected in the observed higher SWR at 1 m/s, as compared to that at 2 m/s.

3. The SWR increases rapidly when the abrading particle size increases between 20 to 30 $\mu$m, which has been attributed to the significant role of microcutting in this range of abrading particle size. However, the magnitude of the increase is less for the composite because of enhanced contribution of delamination wear.
4. The coefficient of friction during abrasion of the composite is observed to lie in the range of 0.45 to 0.75 under various test conditions, but the variation trend of the coefficient of friction with load or abrading particle size is contrary to those observed for tests where sliding is not repeated on the same track. The observed trend of reduced friction with an increase in load or abrading particle size is also attributed to the accumulation of wear debris and the consequent change in the mechanism of wear.
5. In addition to microcutting, abrasion of the composite is observed to take place also by delamination caused by propagation of cracks from the rubbing surface to subsurface through the fly ash–matrix interface and the interfaces of silicon particles which are more in a composite possibly due to chemical reaction of fly ash particles with the molten base alloy during processing.
6. The wear coefficient in both the base alloy and the composite indicates contribution of three-body wear during the tests performed in the present investigation.

## ACKNOWLEDGMENTS

The financial support of the Electric Power Research Institute is gratefully acknowledged. Also, the authors would like to thank Drs. S. Bhattacharyya, B.N. Keshavaram, and N. Nath for discussions of this study and Mr. T. Phillips for assistance with the equipment.

## REFERENCES

1. N.F. Dean, A. Mortensen, and M.C. Flemings: *Metall. Trans. A*, 1995, vol. 26A, pp. 2141-53.
2. S.C. Tjong, H.Z. Wang, and S.Q. Wu: *Metall. Trans. A*, 1996, vol. 27A, pp. 2385-89.
3. F.M. Hosking and F.F. Portillo: *J. Mater. Sci.*, 1982, vol. 17, pp. 477-98.
4. P.K. Rohatgi, Y. Liu, and T.L. Barr: *Metall. Trans. A*, 1991, vol. 22A, pp. 1435-41.
5. J. Zhang and A.T. Alpas: *Scri. Metall.*, 1992, vol. 26, pp. 505-09.
6. N. Saka, N.K. Szeto, and T. Ertürk: *Wear*, 1992, vol. 157, pp. 339-57.
7. K.J. Bhansali and R. Mehrabian: *JOM*, 1982, vol. 349, pp. 30-34.
8. D. Das, S.V. Prasad, and T.R. Ramachandran: *Wear*, 1989, vol. 133, pp. 173-87.
9. P.K. Rohatgi: *JOM*, 1994, Nov., pp. 55-58.
10. P.K. Rohatgi, R.Q. Guo, B.N. Keshevaram, and D. Golden: *Trans. Am. Foundrymen's Soc.*, 1995, vol. 103, pp. 575-79.
11. D. Golden: *EPRI J.*, 1994, Jan./Feb., pp. 46-49.
12. P.K. Rohatgi, P. Huang, R. Guo, B.N. Keshevaram, and D. Golden: *Proc. 5th CANMET/ACI Int. Conf. on Fly Ash, Silica Fume, Slag and Natural Pozzolans in Concrete*, V.M. Malhotra, ed., American Concrete Institute, Detroit, MI, 1995, pp. 459-78.
13. N.P. Suh: *Tribophysics*, Prentice-Hall Inc., Englewood Cliffs, NJ, 1986, pp. 282-84.
14. S.V. Prasad, P.K. Rohatgi, and T.H. Kossel: *Mater. Sci. Eng. A*, 1986, vol. 80, pp. 213-20.
15. P. Rohatgi and R. Asthana: *JOM*, 1991, May, pp. 35-41.
16. A.G. Wang and I.M. Hutching: *Mater. Sci. Technol.*, 1989, vol. 5, pp. 71-76.
17. A. Alahelisten, F. Bergman, M. Olsson, and S. Hogmark: *Wear*, 1993, vol. 165, pp. 221-26.
18. H.C. Sin, N. Saka, and N.P. Suh: *Wear*, 1979, vol. 55, pp. 163-90.
19. E. Rabinowicz: *Friction and Wear of Materials*, John Wiley and Sons, New York, NY, 1965, pp. 168-69.